New spectral templates for rhodopsin and porphyropsin visual pigments

Zoran Gačić[1,*], Branislav Mićković[1], Luka Gačić[2] and Ilija Damjanović[3]

[1] *Institute for Multidisciplinary Research, University of Belgrade*, Kneza Višeslava 1, Belgrade, 11000, Serbia

[2] *Faculty of Agriculture, University of Belgrade*, Nemanjina 6, 11080, Belgrade – Zemun, Serbia

[3] *Institute for Problems of Information Transmission, Russian Academy of Science*, Ermolova St. 19, Moscow, 101447, Russia

***Corresponding author**: zorga@imsi.rs

Abstract: A four-parameter model of spectral sensitivity curves was developed. Empirical equations were designed for A_1- and A_2-based visual pigments with the main α-band maximum absorptions ($λ_{max}$) from 350 nm, near the ultraviolet, up to 635 nm in the far-red part of the spectrum. Subtraction of the α-band from the full absorbance spectrum left a "β-band" described by a $λ_{max}$-dependent Gaussian equation. Compatibility of our templates with A_1- and A_2-based spectra was tested on the electroretinographic (ERG-derived) scotopic action spectra recorded in dogfish shark, eel, Prussian carp and perch. To more precisely estimate the accuracy of our model, we compared it with widely used templates for visual pigments. There was almost no difference between the tested models in fitting the above-mentioned spectral data. One of the advantages of our model is that in the fitting of spectral sensitivity data it uses non-transformed wavelengths and the shape of the curve remains the same for a broad range of $λ_{max}$ values. Compared to multiparameter templates of other authors, our model was designed with fewer (four) parameters, which we believe can bring us closer to understanding the true nature of the absorption curve.

Keywords: spectral sensitivity; electroretinography (ERG); rhodopsin; porphyropsin; fish

INTRODUCTION

Dartnall's [1] fundamental idea that the absorption spectra of all visible pigments can be described by a simple pattern or a "nomogram" is based on the assumption that all absorbance curves of visible pigments have the same basic shape when the frequency scale (c/α) is applied to the abscissas, and only the wavelength at which the maximum absorption is recorded is changed. However, when it comes to spectral sensitivity, Dartnall's findings do not correspond to experimental data obtained for a wider spectrum [2]. Therefore, Ebrey and Honig [2] made an improved version of the nomogram that covered three categories of wavelengths, short, medium, and long wavelengths, for both vitamin A_1- and vitamin A_2-based visual pigments. Almost at the same time, Metzler and Harris [3] reported the analytical expression derived from the lognormal function, which accurately fitted the experimental absorbance spectra. Dawis [4] approximated the log absorbance curves with a polynomial expression (of the 8th degree), with different parameters for the three wavelength ranges. Barlow [5] proposed that the unchanged form of the spectral sensitivity curve could be obtained by plotting the spectra as a function of $λ^{1/4}$–$λ_{max}^{1/4}$. Later, Maximov [6] applied Barlow's transformation and used a combination of trigonometric and exponential functions for the A_1 and A_2 models of the spectral sensitivity curves. In another series of publications, the spectral sensitivity was modeled as a function of frequency [7-9]. It was shown that the frequency normalization, ν/ν max (the Mansfield-MacNichol (MM) normalization), leaves the shape of the spectral sensitivity curves unchanged for A_1 pigments. Stavenga et al. [10] used the MM normalization approach to obtain a new estimate of the common spectral template. They concentrated on fitting the absorbance spectrum that was obtained by Partridge and de Grip [11] for bovine rhodopsin. The exception is the maximum absorption at short wavelengths [12]. On the other hand, for A_2 pigments, by normalizing the frequency, the models do not change the shape of all wavelengths even when the maximum

is at long wavelengths. Lamb [13] attempted to examine further the applicability of the MM normalization to photoreceptor spectral sensitivity curves, especially on the long-wavelength region where both psychophysical and electrophysiological experiments allow for detecting extremely low levels of response. Govardovskii [14] adopted Lamb's [13] formulation with a different set of constant parameter values, to provide a good fit for pigments peaking at intermediate and short wavelengths. This retains the main properties of the template, at the same time enabling it to reproduce the spectral narrowing observed in pigments at short and long wavelengths.

There is still no explanation for the nature of the relationship between the molecular structure and the absorption properties of the visible pigments, so the search for a universal curve is reduced to the empirical search for the curve that best corresponds to the obtained experimental data. Bearing in mind the fact that Lamb-Govardovskii's elegant formula provides the best approximation of invariant shape of spectral sensitivity curves to date, at present most authors use this model [15-18].

Here we designed a model with fewer parameters that could bring us closer to the physical basis of the spectral sensitivity curves. Our new and improved model has altered parameters and needs no transformation to provide a complete description of the absorbance spectra of A_1- and A_2-based visual pigments between 400 nm to far red. In order to more precisely estimate the accuracy of our model we compared it with widely used templates of Maximov [6], Stavenga et al. [10] and Govardovskii et al. [14].

MATERIALS AND METHODS

The complete experimental procedure (including the methods, animals and equipment used) for the data obtained by electroretinography (ERG) has been already described in our previous studies [20-22,31].

Fitting procedures

To enable a computer-aided search for the best-fitting λ_{max}, four procedures were applied to the obtained ERG. The first fitting procedure that was developed in our laboratory employed empirical equations with 3 parameters for fitting the α and β-bands of A1 [20], and 3 parameters for A_2 pigments [21,22].

$$(1)\ S(\lambda) = a \cdot (1 + n)^{-(b+1)/b} \cdot n \cdot (b+1)^{-(b+1)/b}$$

$$n = e^{\frac{[(\lambda + c \cdot \ln(b) - \lambda_{max})]}{c}}$$

The set of parameters in eqn. (1) for A_1-based pigment data was modified; see [20]: a=27.45313, b=0.3809 and c=34.335 and for A_2-based pigments: a=32.8, b=0.2132 and c=46.42.

The short-wave peak remaining after subtraction of the α-band template (1) was fitted with the following Gaussian equation:

$$(2)\ S\beta(\lambda) = A\beta \cdot e^{\{-[\lambda - \lambda m\beta)/d]^2\}}$$

where Aβ is the amplitude of the β-band relative to the α-band, $\lambda_{m\beta}$ is the position of the β-maximum and d is a bandwidth parameter. A_β was fixed at the value 0.22 for A_1-based pigments because of the best fit with bovine rhodopsin spectral sensitivity data (Adj R^2=0.999732724, Fit Standard Error=0.005699731) [11]. The relationships between λ_{max} and the position of the β-maximum ($\lambda_{m\beta}$), and between λ_{max} and d could be approximated as straight lines:

$$(3)\ \lambda_{mb} = 170.1 + 0.339 \cdot \lambda_{max}$$

$$(4)\ d = 34.335 + 0.0086 \cdot \lambda_{max}$$

In the same way as for A_1 pigments, the full absorbance spectrum of A_2-based pigments (Bridges [23] extracts of carp porphyropsin) was broken down into α- and β-bands (Adj R^2= 0.999027941, Fit Standard Error=0.0100105934). We fitted the β-bands with equation (2). A_β was fixed at the value 0.2043 for A_2-based pigments because of the best fit with carp spectral sensitivity data [23]. The relationships between λ_{max} and the position of the β-maximum ($\lambda_{m\beta}$) could be approximated with a straight line (eqn. 5), but the relationship between λ_{max} and d required a second-order approximation (6), similarly to the model of Govardovskii [14].

$$(5)\ \lambda_{m\beta} = 217.6 + 0.277\lambda_{max}$$

$$(6)\ d = 419 - 1.538\lambda_{max} + 0.001583\lambda_{max}^2$$

Equations (1)-(6) provide a complete description of the absorbance spectra of A_1- and A_2-based visual pigments, between 400 nm to far red. Bearing in mind that the eyes of freshwater fish possess a mixture of A_1- and A_2-based visual pigment [24], we combined both fitting procedures of our spectral sensitivity data to find the best fit that provides the percent of A_1-based photopigment.

The second procedure was based on the widely used formula of Lamb [13]:

$$S_{(\lambda)} = \frac{1}{\exp\left[A(a-x)+B(b-x)+C(c-x)+D\right]}$$

where $x=\lambda_{max}/\lambda$, with the parameters proposed by Govardovskii [14]: $A = 69.7$, $a = 0.88$, $B = 28$, $b = 0.922$, $C = 014.9$, $c = 1.104$, $D = 0.674$, for the α-band of bovine rhodopsin (main absorbance band of visual pigments). Mansfield normalization was used [7]; absorbance spectra were plotted on a normalized frequency to provide Dartnall's fundamental hypothesis that the absorbance spectra had a closely similar shape when plotted on a frequency scale (c/λ) at the basis of his nomogram [1].

The third procedure was based on Stavenga [10], who proposed that a complete visual pigment spectrum can be resolved in several bands. Estimation of their precise location and shape will be facilitated by fitting first the α-band and subsequently the β-band. The bands can be fitted appropriately with lognormal functions:

$$\alpha i = A_i \exp[-\alpha_{0i}x_i^2(1+\alpha_{1i}x_i+\alpha_{2i}+\alpha_{2i}x_i^2)],$$

where $i=\alpha, \beta...$, and $x_\alpha=\log(\lambda/\lambda_{max\lambda})$, $x_\beta=\log(\lambda/\lambda_{max}\beta)...$, so that the final spectral sensitivity curve is the sum of α, β... bands:

$$S_{(\lambda)} = \Sigma\alpha_i(\lambda) = \alpha(\lambda)+\beta(\lambda)+...$$

The 4th procedure was based on a combination of trigonometric and exponential functions which use Barlow's finding that the width of the major absorption band of light-sensitive pigments with various λ_{max} remains constant if it is measured not as the scale of frequencies but as the scale of $\lambda^{1/4}- \lambda_{max}^{1/4}$, for an A_1-based pigment [6]:

$$S_{(\lambda)} = e^{(-\psi^2 \bullet \xi^2)}$$

$$\xi = 6 + 6\psi + \frac{2}{3}\arctan(21\psi + 6)$$

and

$$\xi = 5 + 6\psi + \frac{2}{3}\arctan(21\psi + 6),$$

for an A_2-based pigment, where $\psi=\lambda^{1/4}-\lambda_{max}^{1/4}$.

These four procedures were applied to both the b-wave and the late receptor potential (LRP)-derived spectral sensitivity data.

RESULTS

Intensity-amplitude relations

The regularity of the intensity-amplitude relation for the b-wave and the iodate unmasked LRP for eels and dogfish sharks has been checked by fitting the experimental data with the basic model (see Fig. 1 top panel) [19,25]:

(7) $V_o = I^\alpha / (I_o^\alpha + I^\alpha)$,

where V_o is the normalized voltage (V/V_{max}) of the ERG signal (b-wave or LRP), I_o is the stimulating light intensity corresponding to $V_o = 1/2$, and the exponent a is a constant (see Fig. 1). Fitted log-sigmoids were used for calculating the threshold values on which to base the spectral sensitivity determinations.

The choice of the threshold criterion for sensitivity determinations is irrelevant only when $V_o/log\ I$ profiles are strictly parallel. Although the variations in parameter a were small, a signal amplitude equal to 10% of the largest response, obtained with light stimuli of the most effective wavelength, was adopted as the threshold criterion.

The data that were included in the evaluation of the characteristics of the goldfish and perch retina were subsequently tested using eqn. (7) (Fig. 1, bottom panel goldfish-left, perch-right).
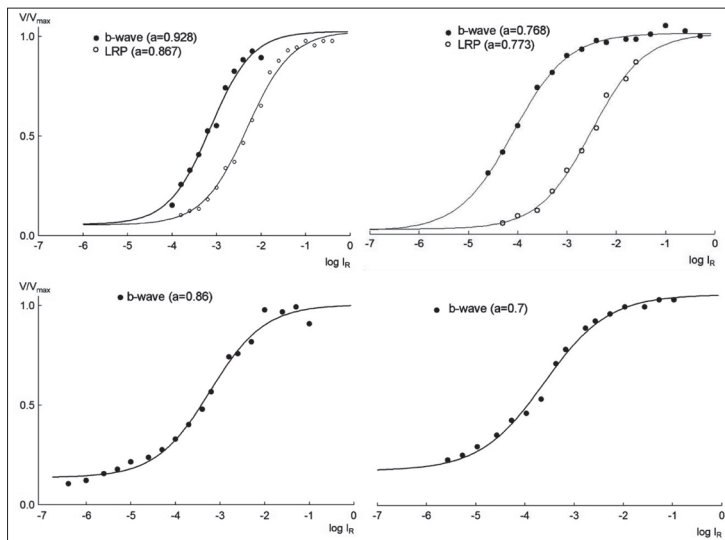
Fig. 1. Top panel: LRP (open circles) and b-wave (closed circles) amplitude/intensity relations in silver eel (left) and dogfish (right). Preparations: *in situ* eyecup of the eel, isolated eyecup of the dogfish. In both cases LRP was unmasked by sodium iodate. Stimulus wavelength: 500 nm. IR: relative flash intensity. Unattenuated, the energy flux delivered by the test field was of the order of 2×10^{-2} mW/cm^2. Fitting according to Eqn. (7). Bottom panel: b-wave (closed circles) amplitude/intensity relation in a Prussian carp (left) and a perch (right). Preparations: *in situ* eyecup. Stimulus wavelength: 520 nm (Prussian carp) and 545 nm (perch). The maximum unattenuated light intensity of the beam from the 50 W tungsten-halogen lamp was 282 μW/cm^2. Fitting according to Eqn. (7).

ERG amplitudes were acquired by using an incremental stimulus with light stimuli of the most effective wavelength. The measured slope of the sigmoid curve for the goldfish was $a=0.86$ with a standard sigmoid deviation of 0.02. The threshold values for perch were determined from the intensity-response functions obtained with light stimuli of the most effective wavelength (545 nm, slope: $a=0.7\pm0.05$). In no case were the variations of parameter a in correlation with the wavelength. A signal amplitude equal to 65 μV was adopted as the threshold criterion; it is approximately 10% of the greatest response obtained with light stimuli of the most effective wavelength. In no case were there indications of the division of the amplitude-intensity curves into two (rod and cone) S-shaped branches of the type described in the case of the isolated frog retina [26].

Action spectra

The absorbance spectrum of bovine rhodopsin measured by Partridge and De Grip [11] from highly purified extracts provides a curve of reference quality for
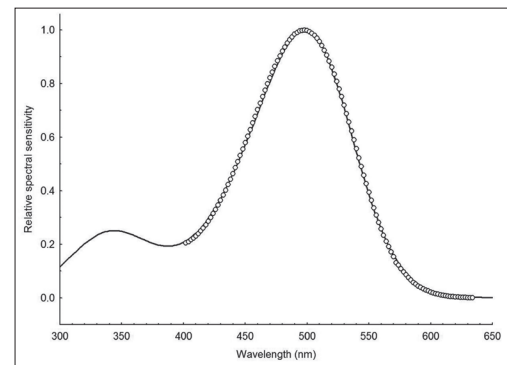

Fig. 2. Absorbance spectrum of bovine rhodopsin (open circle) measured by Partridge and De Grip [11] and fitted with our model for A_1-based pigments (solid line).
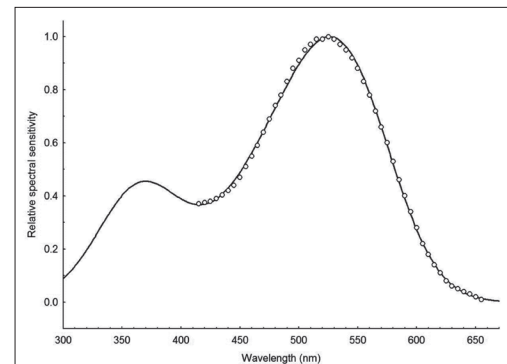

Fig. 3. Absorbance spectrum recorded from carp porphyropsin (open circle) and extract by Bridges [23] fitted with our model for A_2-based pigments (solid line).

A_1 pigments (Fig. 2). For A_2 pigments, the spectrum recorded from carp porphyropsin extract by Bridges [23] could be an acceptable standard (Fig. 3).

We tested our model (equations 1-6) for A_1 pigments on our scotopic ERG data for the small-spotted dogfish shark (*S. canicula*) and silver eels (*A. anguilla*), and also on Danio cone [27] and frog rod [1] data (Fig. 4). Also, we tested the model for A_2 pigments on our scotopic ERG data of perch, Prussian carp and yellow eel, and additionally on the carp rod spectrum [23] (Fig. 5). As can be seen from Fig. 4 data for Danio cones with λ_{max} values in short-wavelength that did not fit well, the Govardovskii comment [14] about data quality of small fish cones applies to our template.

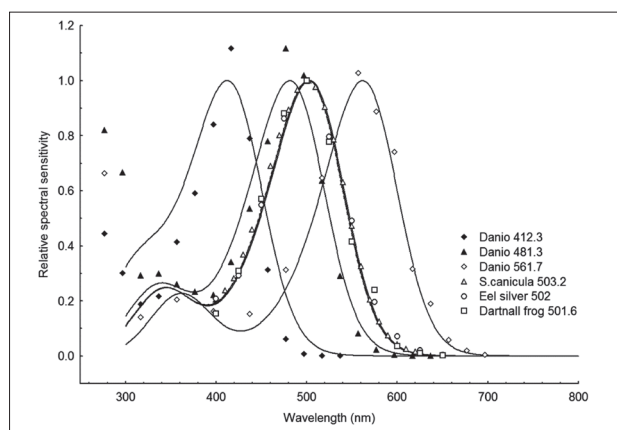We also tested all spectral sensitivity data, either by the procedure of Lamb-Govardovskii, or using Stavenga,

Fig. 4. A1 pigment-based spectral sensitivity of the giant danio (*Devario aequipinnatus*, [27]) short wave cone – ◆, middle wave cone – ▲, long wave cone – ◊; scotopic ERG data of dogfish-shark [20] – △, and silver eel [31] – ○; Dartnall's data for the frog rod spectrum [1] – □. Solid lines – our model for A1 based pigments.
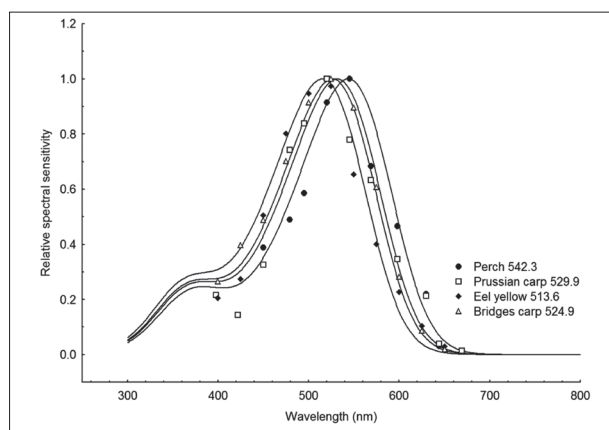

Fig. 5. A2 pigment-based spectral sensitivity of the Prussian carp (Carassius gibelio, [22]) – ●, yellow eel [31] – □, perch (Perca fluviatilis) (all scotopic ERG data; [21]) – ◆, and carp rod spectrum [23] – △. Solid lines – our model for A2-based pigments.

Table 1. λ_{max} values (*nm*) obtained by means of various fitting methods based on A1 pigments, A2 pigments and a mixture of A2 and A1 pigments (spectral curve models: our new and improved model – the first three columns, Lamb-Govardovskii model [14], Stavenga model [10] and Maximov model [6]).

Retina	Gačić A1 λ_{max}	Gačić A2 λ_{max_x}	Gačić A2/A1 λ_{max}	Lamb-GovA1 λ_{max}	Lamb-GovA2 λ_{max}	Lamb-GovA2/A1 λ_{max}	Stavenga A1 λ_{max}	Stavenga A2 λ_{max}	Maximov A1 λ_{max}	Maximov A2 λ_{max}
Frog [1]	501.6	499.9	501.3	501.6	498.3	501.4	501.2	496.7	500.4	499
Eel silver [31]	502	498.5	501.6	502	498.2	501.7	501.6	496.5	500.7	498.6
Dogfish shark [20]	503.2	500.0	500.4	500.6	498	501.4	501.2	493.1	499.7	498.6
Giant danio [27]	561.7	557.2	560.2	558.5	554.7	554.2	558.6	559.6	555	545.9
Giant danio [27]	481.3	479.5	481.2	482.8	480.9	491.7	480	478.4	484	475.9
Giant danio [27]	412.3	412.8	406.5	414.8	410.1	414.2	408.4	409.3	411.4	407.6
Perch [21]	541.5	542.3	542.6	542.8	541.4	541.9	542.3	538.8	541.2	541.9
Carp [23]	525.4	524.9	526.5	527.3	525.1	523	518.7	522.3	525.9	523.9
Prussian carp [22]	524.3	529.9	529.9	526.6	530.0	530.1	525.1	522.6	527.7	528.2
Eel yellow [31]	513.9	513.6	514.1	514.5	512.7	514	514.5	511.1	513.3	512.2

Maximov and our procedure. All fitting procedures for A_1 pigments (Table 1) gave relatively small differences between λ_{max} values for frog [1] (500.4-501.6 nm), silver eel (500.7-502 nm), and for dogfish shark (499.7-503.2 nm). The spectral sensitivity curves obtained in short-, medium- and long-wavelength cones [27] of giant danio (*Devario aequipinnatus*), which belonged to A_1-based photopigments, were simultaneously fitted with all models, giving differences between λ_{max} values for short-wavelength 408.4-414.7 nm, for medium-wavelength 480-484 nm, and for long-wavelength 555 to 561.7 nm cones.

The differences between λ_{max} values simultaneously fitted with our, Lamb-Govardovskii's, Stavenga's

and Maximov's models for A_2-based pigments (Table 1) of carp [23], Prussian carp, yellow eel and perch where relatively small (carp 522.3-525.1 nm, Prussian carp 522.6-530 nm, yellow eel 511.1-513.6 nm, perch 538.8-542.9 nm).

Relationship between λ_{max} of the β-band and λ_{max} of the α-band

Fig. 6. shows the relation between the λ_{max} of the β-band to the λ_{max} of the α-band. Using different fitting methods for A_1- and A_2-based pigments, we showed that the data for A_1- and A_2-based pigments lies on the regression line almost ideally in the case of our templates
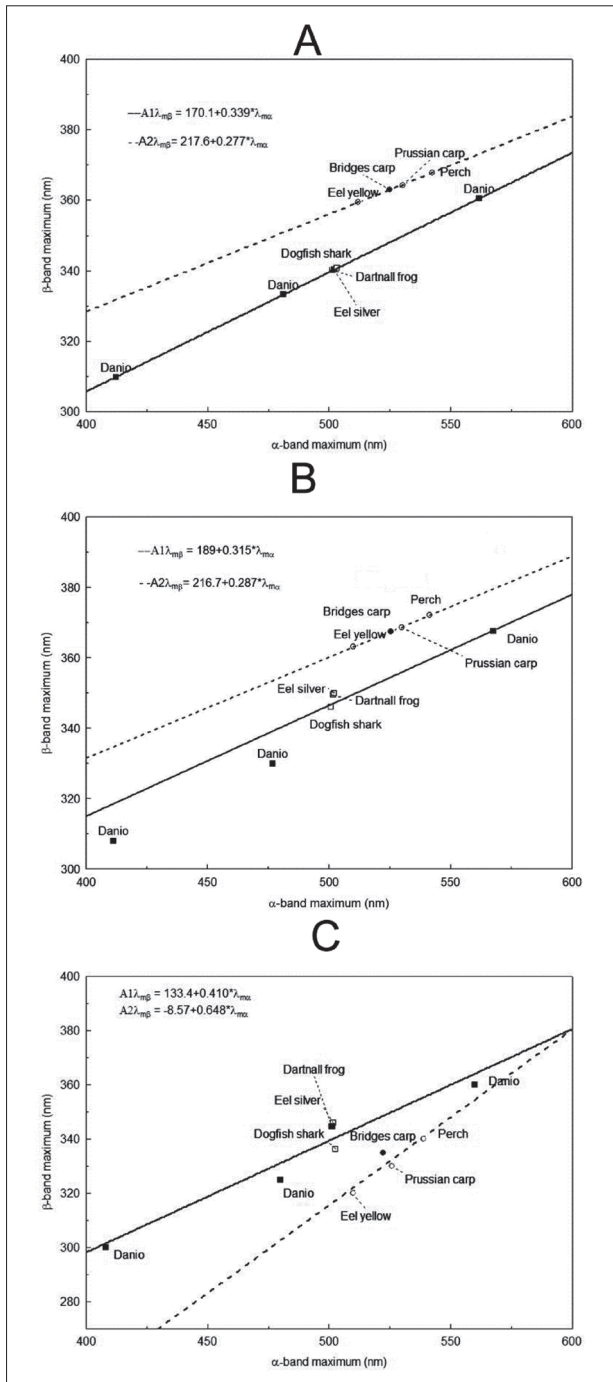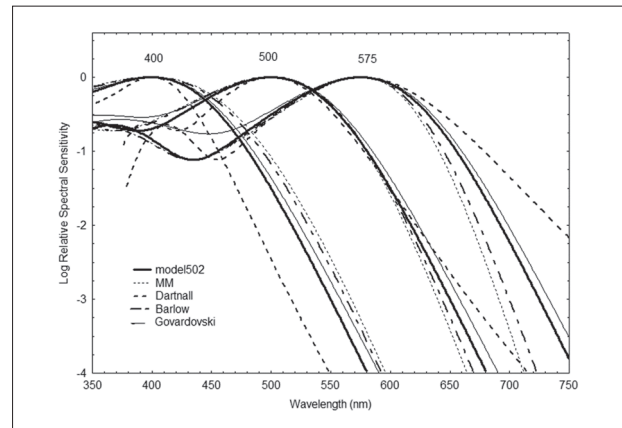
Fig. 7. Relationship between different transformations (Govardovskii improvement of Mansfield normalization, Mansfield normalization, Barlow $\lambda^{1/4}-\lambda^{1/4}_{max}$, Dartnall's rule and our model) applied to the same basic rhodopsin curve. The absorbance curve of rhodopsin-500 (thick solid line) was generated by eqn. (1) in the text and then transformed to λ_{max}=400 and =575 nm. Thick dotted hyphenated line – Dartnall's rule (c/λ); thin solid line – Govardovskii's improvement of Mansfield's normalization; thin hyphenated line – Mansfield's normalization (λ_{max}/λ); dotted line – Barlow's transformation ($\lambda^{1/4}-\lambda^{1/4}_{max}$); thick solid line – this study.

Fig. 6. Spectral position (λ_{max}) of the β-band as a function of the λ_{max} of the α-band for several visual pigments fitted with our model (A), Govardovskii's (B) and Stavenga's models (C). Filled circles: Bridges' [23] data for carp rod porphyropsin. Open circles: A_2-based scotopic ERG data for the Prussian carp (*Carassius gibelio*, [22]), yellow eel [31] and perch (*Perca fluviatilis,* [21]). Filled quadrate: A_1-based cone pigments of another teleost, giant danio and Dartnall's data for frog rhodopsin [1]. Open quadrate: A_1-scotopic ERG data for silver eel [31] and dogfish-shark [20]. Equations for the fits to the data are given in corresponding panels.

(A_1- and A_2-based). The data were successfully fitted with the Govardovskii model as well (for A_2-based pigments they were the same as in our model), but the Stavenga model gave a higher level for the λ_{max} of the β-band for A_1-based pigments, thus the position of the regression line was reverse when compared to our model and the model proposed by Govardovskii.

Transformation rule

Fig. 7. shows the comparison between the four transformations and our model (model 502) when applied to the same basic rhodopsin curve generated by eqn. (1) and then transformed to λ_{max} =400 and =575 nm. Our model for an A_1-based pigment describes spectral sensitivity data in a satisfactory manner, thus we used it as the basis for the comparison (thick solid line in Fig. 7). Dartnall's original transform (shape invariance in the frequency scale) generates curves that are too wide for the long-wave visual pigments and too narrow for the short-wave pigments. The $\lambda^{1/4}-\lambda^{1/4}_{max}$ transform originally suggested by Barlow [5] is wider both at short and long wavelengths. The MM transform (shape invariance in the normalized wavelength/frequency scale) is wider for λ_{max} <465 nm and narrow for >575 nm pigments. Govardovskii's improvement of the MM

transform is slightly wider at all wavelengths when compared to our model.

DISCUSSION

The slope (parameter *a*) of the intensity-amplitude of the log sigmoid response that determines the response dynamics in our small spotted dogfish shark, eel, Prussian carp and perch preparations, were also within the framework of those registered for other animals and other electrophysiological signals [19,25,28]. The parameter for eels had a value of 0.7-0.8. In Prussian carp, the variation in the log-sigmoid angle was much higher (0.55-1). The slopes for Prussian carp covered the range of 3-4 logarithmic intensity stimulus units, which is in accordance with the extent obtained by intracellular exploration of frog rods [29] or the responses obtained from horizontal cells of rays [19].

In our previous paper [20], the standard curve for the A_1-based pigment was based on frog spectral sensitivity data obtained by Dartnall [1]. Here, we adopted the absorbance spectrum of bovine rhodopsin measured by Partridge and De Grip [11] from highly purified extracts because it was a significant technical progress since Dartnall. Bridges' [23] extracts of carp porphyropsin served as a standard for A_2-based pigments. The curve based on the rhodopsin is 50% narrower 19.9 nm at the absorption value when compared to the porphyropsin curve (99.6 and 119.5 nm). The disadvantage of changing the shape of the curve in the normalization of the frequency at short wavelengths was solved by model 502 by allowing it to break down the entire spectrum into α- and β-positions [10]. The β-range itself was simply obtained when the α-range was taken away from the complete experimental spectrum, thus covering all the maximum values from 350 nm to far red light.

Our results are based on the data obtained on the fish ERG where the differences between the spectral sensitivity points were about 25 nm. The data fitted well with our templates, based on the highly purified extracts of bovine rhodopsin and extracts of carp, where steps between spectral sensitivity data are 2 nm. The data obtained by microspectrophotometry have the advantage of better fitting because the steps between spectral sensitivity data are only 1 nm, regardless of the

fact that the signal-to-noise ratio must be resolved by different mathematical models. Another disadvantage of our model is that we did not test it on a sufficient number of spectral sensitivity data. For example, Govardovskii et al. [14] tested their model on spectral data collected by microspectrophotometry from 39 different rod and cone types representing amphibians, reptiles, and fishes. Irrespective of all the deficiencies of our model, in estimating the maximum spectral sensitivity there is almost no difference between all of the tested models. Fitted λ_{max} for ERG data of fish possessing pure A_1- or pure A_2-based pigments (dogfish shark, silver eels, perch) were consistent with previously reported data [20; 21; 30; 31; 32]. Fish possess A_1- or A_2-based pigments (rhodopsins and porphyropsins, respectively). Accordingly, the maximum absorption values (λ_{max}) of fish visual pigments are spread over a wide range, from 350 nm near the ultraviolet up to 635 nm in the far-red part of the spectrum. In most cases, porphyropsin is predominant in freshwater fish, while rhodopsin is dominant in marine fish, but many fish species have mixtures of these two pigments, and paired systems of visible pigments that consist of a mixture of rhodopsins and porphyropsins are not unusual in fish. The shift in the spectral sensitivity associated with replacement of A_1/A_2 pigments is prior knowledge [33-36]. When we fitted the spectral sensitivity data with our model for A_2-based pigments, some deviations appeared because Prussian carps and yellow eels possess different mixtures of A_1 and A_2 pigments [22; 31; 37]. Therefore, our fitting procedure gives a nearly optimal estimate for λ_{max} of visual pigments of tested fish. One of the advantages of our model is that in the fitting of spectral sensitivity data, it uses non-transformed wavelengths, with the shape of the curve remaining the same even when the maximum sensitivity is in the short, medium or long wavelengths. It should also be noted that in comparison with the multiparameter formula of Lamb and Govardovskii, our model is designed with fewer (four) parameters, which brings us closer to understanding the true nature of the absorption curve.

REFERENCES

1. Dartnall HJA. The interpretation of spectral sensitivity curves. Br Med Bull. 1953;9:24-30.

2. Ebrey TG, Honig B. New wavelength-dependent visual pigment nomogram. Vis Res. 1977;17:147-51.

3. Metzler DE, Harris CM. Shapes of spectral bands of visual pigments. Vis Res. 1978;18:1417-20.

4. Dawis SM. Polynomial expression of pigment nomograms. Vis Res. 1981;21:1427-430.

5. Barlow HB. What causes trichromacy? A theoretical analysis using comb-filtered spectra. Vis Res. 1982;22:635-43.

6. Maximov VV. Approximation of visual pigment absorbance spectra. Senssornye Sistemy. 1988;2:3-9. Russian.

7. Mansfield RJW. Primate photopigments and cone mechanisms. In: Levine JS, Fein A, editors. The Visual System. New York: Alan Liss; 1985. p. 89-106.

8. Mansfield RJW, Levine JS, Lipetz LE, Oleszko-Szuts S, Macnichol EFJr. Vertebrate visual pigments: Canonical form of the absorbance spectra a-band. Invest Ophthalmol Vis Sci. 1986; 27:193.

9. Macnichol EF. A unifying presentation of photopigment spectra. Vis Res. 1986;26:1543-56.

10. Stavenga DG, Smits RP, Hoenders BJ. Simple exponential functions describing the absorbance bands of visual pigment spectra. Vis Res. 1993; 33:1011-7.

11. Partridge JC, De Grip WJ. A new template for rhodopsin (vitamin A1 based) visual pigments. Vis Res. 1991;31:619-30.

12. Hárosi FI. An analysis of two spectral properties of vertebrate visual pigments. Vis Res. 1994;34:1359-67.

13. Lamb TD. Photoreceptor spectral sensitivities: Common shape in the long-wavelength region. Vis Res. 1995;35(22):3083-91.

14. Govardovskii VI, Fyhrquist N, Reuter T, Kuzmin DG, Donner K. In search of the visual pigment template. Vis Neurosci. 2000;17:509-28.

15. Kondrashev SL. Spectral sensitivity and visual pigments of retinal photoreceptors in near-shore fishes of the Sea of Japan. Russ J Mar Biol. 2010; 36(6):443-51.

16. Shand J, Hart NS, Thomas N, Partridge JC. Developmental changes in the cone visual pigments of black bream *Acanthopagrus butcheri*. J Exp Bio. 2002;205:3661-7.

17. Stavenga DG. On visual pigment templates and the spectral shape of invertebrate rhodopsins and metarhodopsins. J Comp Physiol A Neuroethol Sens Neural Behav Physiol. 2010;196(11):869-78.

18. Lisney TJ, Studd E, Hawryshyn CW. Electrophysiological assessment of spectral sensitivity in adult Nile tilapia *Oreochromis niloticus*: evidence for violet sensitivity. J Exp Bio. 2010;213:1453-63.

19. Dowling JE, Ripps H. S-potentials in the skate retina. Intracellular recordings during light and dark adaptation. J Gen Physiol. 1971;58:163-90.

20. Gačić Z, Damjanović I, Mićković B, Hegediš A, Nikčević M. Spectral sensitivity of the dogfish shark (*Scyliorhinus canicula*). Fish Physiol Biochem. 2007a;33:21-7.

21. Gačić Z, Bajić A, Milošević M, Nikčević M, Mićković B, Damjanović I. Spectral sensitivity of the perch (*Perca fluviatilis*) from the Danube. Arch Biol Sci. 2007b;59:335-40.

22. Gačić Z, Bajić A, Milošević M, Nikčević M, Mićković B, Hegediš A, Gačić L, Damjanović I. Spectral sensitivity of the electroretinogram b-wave in dark-adapted Prussian carp (*Carassius gibelio* Bloch, 1782). Fish Physiol Biochem. 2014;40:1899-906.

23. Bridges CDB. Photopigments in the char of Lake Windermere (*Salvelinus willughbii*, forma autumnalis and forma vernalis). Nature 1967;214:205-6.

24. Powers MK, Easter SS. Wavelength discrimination by the goldfish near absolute visual threshold. Vis Res. 1978;18:1149-54.

25. Naka KI, Rushton WAH. S-potentials from luminosity units in the retina of fish (Cyprinidae). J Physiol. 1966;185:587-99.

26. Zaret WN. The effects of calcium, calcium-chelating drugs and methylxanthines on the vertebrate photoreceptor potential [dissertation]. [New York]: New York University. 1973. 120p.

27. Palacios AG, Goldsmith TH, Bernard GD. Sensitivity of cones from a cyprinid fish (*Danio aequipinnatus*) to ultraviolet and visible light. Vis Neurosci. 1996;13:411-21.

28. Baylor DA, Fuortes MGF. Electrical response of single cones in the retina of the turtle. J Physiol. 1970;207:77-92.

29. Lipton SA, Ostroy SE, Dowling JE. Electrical and adaptive properties of rod photoreceptors in *Bufo marinus*. J Gen Physiol. 1977;70:747-70.

30. Carlisle DB, Denton E J. On the metamorphosis of the visual pigments of *Anguilla anguilla* (L.). J Mar Biol Assoc UK. 1959;38:97-102.

31. Andjus RK, Damjanović I, Gačić Z, Konjević D, Andjus PR. Electroretinographic evaluation of spectral sensitivity in yellow and silver eels (*Anguilla anguilla*). Vis Neurosci. 1998;15:923-30.

32. Cameron NE. The photopic spectral sensitivity of a dichromatic teleost fish (*Perca fluviatilis*). Vis Res. 1982;22:1341-8.

33. Dartnall,HJA, Lander MR, MUNZ, W. Periodic changes in the visual pigment of a fish. In: Cristiansen B, Buchmann B, editors. Progress in Photobiology. Amsterdam: Elsevier; 1961. p. 203-13.

34. Allen DM. Photic control of two visual pigments in fish. Vis Res. 1971;11:1077-112.

35. Loew ER, Dartnall HJA. Vitamin A1/A2 based visual pigment mixtures in cones of the rudd. Vis Res. 1976;16:891-6.

36. Whitmore AV, Bowmaker JK. Seasonal variation in cone sensitivity and short-wave absorbing visual pigments in the rudd *Scardinius erythrophthalmus*. J Comp Physiol A. 1989;166:103-15.

37. Beatty DD. Visual pigments of the American eel *Anguilla rostrata*. Vis Res. 1975;15:771-6.